Low Temperature Physics

RESEARCH ARTICLE | OCTOBER 01 2024

B3LYP and B3PW computations of $BaSnO_3$ and $BaZrO_3$ perovskite (001) surfaces FREE

R. I. Eglitis; A. I. Popov; Ran Jia; S. P. Kruchinin; I. Derkaoui; M. A. Basyooni-M. Kabatas

Low Temp. Phys. 50, 905–910 (2024)
https://doi.org/10.1063/10.0028638

Low Temperature Physics ARTICLE pubs.aip.org/aip/ltp

B3LYP and B3PW computations of $BaSnO_3$ and $BaZrO_3$ perovskite (001) surfaces

Cite as: Fiz. Nizk. Temp. **50**, 1005–1011 (October 2024); doi: 10.1063/10.0028638
Submitted: 19 August 2024

R. I. Eglitis,[1,a)] A. I. Popov,[1] Ran Jia,[1,2] S. P. Kruchinin,[3] I. Derkaoui,[4] and M. A. Basyooni-M. Kabatas[5]

AFFILIATIONS

[1]Institute of Solid State Physics, Kengaraga 8, Riga LV 1063, Latvia
[2]Laboratory of Theoretical and Computational Chemistry, Institute of Theoretical Chemistry, Jilin University Changchun 130023, PR China
[3]Bogolyubov Institute for Theoretical Physics of the National Academy of Sciences of Ukraine, Kyiv 03143, Ukraine
[4]Laboratory of Solid State Physics, Faculty of Sciences Dhar el Mahraz, University Sidi Mohammed Ben Abdellah P.O. Box 1796, Atlas Fez 30000, Morocco
[5]Dynamics of Micro and Nano Systems Group, Department of Precision and Microsystems Engineering Delft University of Technology, Mekelweg 2, 2628 CD Delft, The Netherlands

[a)]**Author to whom correspondence should be addressed:** rieglitis@gmail.com

ABSTRACT

By means of the B3LYP and B3PW hybrid exchange-correlation functionals, as it is included in the CRYSTAL computer code, we performed *ab initio* computations for $BaSnO_3$ and $BaZrO_3$ perovskite (001) surfaces. For $BaSnO_3$ and $BaZrO_3$ perovskite (001) surfaces, with a few exceptions, all atoms of the upper surface layer relax inwards, all atoms of the second surface layer relax outwards, and all third layer atoms, again, relax inwards. The relaxation of $BaSnO_3$ and $BaZrO_3$ (001) surface metal atoms for upper two surface layers, for both BaO and BO_2-terminations, as a rule, are considerably larger than the relaxation of relevant oxygen atoms. The BaO (1.30 eV) and ZrO_2-terminated (1.31 eV) $BaZrO_3$ (001) surface energies are almost equal. The $BaZrO_3$ perovskite BaO (4.82 eV) and ZrO_2-terminated (4.48 eV) (001) surface Γ-Γ band gaps are reduced regarding the respective bulk Γ-Γ band gap value (4.93 eV). The B–O chemical bond populations in $BaSnO_3$ and $BaZrO_3$ perovskite bulk always are smaller than near their SnO_2 and ZrO_2-terminated (001) surfaces, respectively.

1. INTRODUCTION

Surface and (001) interface phenomena, happening in the ABO_3 perovskites, are crucial topics in the present-day physics.[1–15] The $BaSnO_3$ (BSO) and $BaZrO_3$ (BZO) perovskites are the members of ABO_3-class perovskite oxides. They carry a colossal quantity of technologically important applications, such as actuators, charge storage devices, capacitors and many others.[16–22] For that reason, in the last 25 years, $BaZrO_3$ and $BaSnO_3$ (001) surfaces were worldwide explored both experimentally as well as theoretically.[23–41] Nevertheless, for *ab initio* calculations of BSO and BZO (001) surfaces, mostly the density functional theory (DFT)-based methods were used, which very strongly underestimate the BSO and BZO experimental Γ-Γ band gaps.

According to the X-ray diffraction analysis (XRD) measurement results obtained by Janifer *et al.*,[42] barium stannate (BSO) is the single-phase cubic perovskite.[42,43] Moreover, BSO has the wide optical band gap equal to 3.1 eV,[42,43] and the cubic lattice parameter *a* indentical to 4.119 Å.[42,43] According to Knight,[44] the BZO perovskite is cubic at all measured temperatures inside the temperature range from 4.2 K till 450 K.[44] Namely, BZO always has the cubic ABO_3 perovskite structure with the symmetry group $Pm\bar{3}m$.[44] Thereby, the experimentally measured BZO Γ-Γ band gap is equal to 5.3 eV in its high-symmetry cubic structure.[45]

As it is well known, the *ab initio* Hartree–Fock (HF) method,[46] as a rule, systematically overestimates the band gap of complex oxide materials. For example, our *ab initio* HF computed Γ-Γ band gap for BZO perovskite bulk is equal to 12.96 eV.[47] Just opposite, from another side, the DFT-based methods, as a general rule, strongly underestimate the band gap of solids. To give an example, our PWGGA computed BZO bulk Γ-Γ band gap is equal to 3.24 eV.[47] The best possible agreement with the experiment, according to our computations for BZO bulk Γ-Γ band gap, gives

the hybrid exchange-correlation functional, such as B3PW and B3LYP. Namely, our B3PW computed BZO bulk Γ-Γ band gap is equal to 4.93 eV,[47] whereas our B3LYP computed BZO bulk Γ-Γ band gap is equal to 4.79 eV,[48] in almost a perfect agreement with the available experimental data for the bulk Γ-Γ band gap of 5.3 eV.[45] In this paper, we carried out most of our BSO and BZO (001) surface computations utilizing the hybrid exchange-correlation functionals B3LYP and B3PW, which unify 20% of the HF and 80% of the density functional Hamiltonian, as it is put into action in the CRYSTAL code.[49]

2. COMPUTATION METHOD AS WELL AS (001) SURFACE MODELS

For our DFT-B3PW or DFT-B3LYP computations, we engaged the CRYSTAL computer programme.[49] The trump card of the CRYSTAL code[49] is its capability to compute confined 2D (001) SZO and BZO perovskite slabs without imposed periodicity along the z axis.[49] In order to engage the linear combination of atomic orbitals approach,[49] it is mandatory to take advantage of the optimized basis sets (BS).[49] The BS for Sn and Zr we took from the CRYSTAL code BS library.[49] The optimized BS for BTO perovskite was developed in Ref. 50. All our BSO and BZO perovskite bulk as well as (001) surface computations were carried out by means of the B3PW[51,52] or B3LYP[53] hybrid exchange-correlation functionals. We carried out the reciprocal space integration by checking out the Brillouin zone for the five-atom BSO and BZO perovskite cubic unit cell by employing the $8 \times 8 \times 8$ times increased Pack–Monkhorst net[54] for the BSO and BZO perovskite bulk as well as the $8 \times 8 \times 1$ times increased mesh for their (001) surfaces. The ABO_3 perovskite (001) surfaces were illustrated adopting 2D slabs (Figs. 1 and 2).

Specifically, in order to compute BSO and BZO perovskite (001) surfaces, we studied slabs formed of nine alternating BO_2 and BaO layers (Figs. 1 and 2). The mirror symmetries of the slabs were detained with regard to their center. Our B3LYP and B3PW computed containing 23-atom BSO and BZO slabs with BO_2-terminated surfaces as well as the 22-atom slab with BaO-terminated surfaces are illustrated in Figs. 1 and 2, respectively. They have unit-cell equations $A_4B_5O_{14}$ and $A_5B_4O_{13}$, respectively. The definitions of the interplane separations Δd_{12}, Δd_{23} and the surface rumpling s are illustrated in Fig. 1.

The first step for the BSO and BZO perovskite (001) surface energy computations is to compute the relevant cleavage energies. Our B3LYP or B3PW computed BSO or BZO cleavage energies are equally distributed between the created (001) surfaces. In our carried out BSO and BZO perovskite (001) surface cleavage energy computations, nine-layers BaO and BO_2-terminated (001) slabs accommodate together 45 atoms, which corresponds to nine ABO_3 perovskite unit cells:

$$E^{\mathrm{unr}}_{\mathrm{surf}}(\mathrm{AO}+\mathrm{BO_2}) = \frac{1}{4}\left[E^{\mathrm{unr}}_{\mathrm{slab}}(\mathrm{AO}) + E^{\mathrm{unr}}_{\mathrm{slab}}(\mathrm{BO_2}) - 9E_{\mathrm{bulk}}\right], \quad (1)$$

where $E^{\mathrm{unr}}_{\mathrm{slab}}(\mathrm{AO})$ and $E^{\mathrm{unr}}_{\mathrm{slab}}(\mathrm{BO_2})$ are the unrelaxed AO and BO_2-terminated (001) surface ABO_3 perovskite nine-layer slab total energies; E_{bulk} denotes the total energy for the BSO or BZO perovskite bulk unit cell, which contains five atoms. In the next step, the AO as well as BO_2-terminated nine-layer (001) slab relaxation

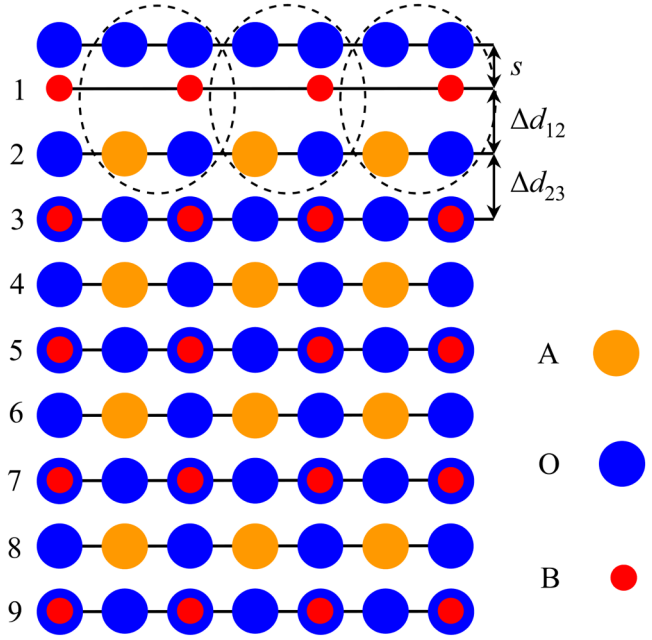

FIG. 1. Outline of the BO_2-terminated (001) surface of ABO_3-type perovskite enclosing nine atomic layers.

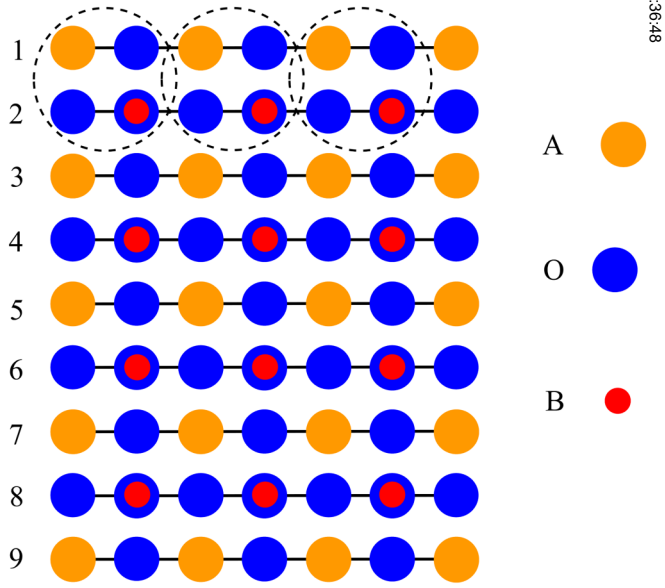

FIG. 2. Outline of the AO-terminated (001) surface of ABO_3-type perovskite enclosing nine atomic layers.

energies were computed:

$$E_{\mathrm{rel}}(\lambda) = \frac{1}{2}\left[E^{\mathrm{rel}}_{\mathrm{slab}}(\lambda) - E^{\mathrm{unr}}_{\mathrm{slab}}(\lambda)\right], \quad (2)$$

where λ is BaO or BO_2; $E^{\mathrm{rel}}_{\mathrm{slab}}(\lambda)$ is the computed total energy for both sides relaxed BaO or BO_2-terminated BSO or BZO (001) slab; $E^{\mathrm{unr}}_{\mathrm{slab}}(\lambda)$ is the computed total energy for unrelaxed BaO or BO_2-terminated BSO or BZO perovskite (001) slab. In the end, the BaO or BO_2-terminated ABO_3 perovskite (001) surface energy should be computed by means of the following equation:

$$E_{\mathrm{surf}}(\lambda) = E^{\mathrm{unr}}_{\mathrm{surf}}(\mathrm{AO} + \mathrm{BO}_2) + E_{\mathrm{rel}}(\lambda). \quad (3)$$

3. MAIN RESULTS FOR BSO AND BZO PEROVSKITE BULK AND (001) SURFACES

3.1. BSO and BZO bulk results

As the takeoff of our B3PW, B3LYP, HF, and PWGGA computations, we computed the theoretical bulk lattice constants for BSO and BZO perovskites[32,47,48,55,56] (Table I). We coordinated our computation results with the existing experimental data[55,56] (Table I). We carried out the theoretical bulk lattice constant computations also using the *ab initio* Hartree–Fock (HF) method.[46] For *ab initio* DFT bulk lattice constant calculations, we selected the generalized gradient approximation suggested by Perdew and Wang (PWGGA).[50] As we can see from Table I, our B3LYP (4.107 Å) and PWGGA (4.107 Å) computed BSO bulk lattice constants are in the best possible agreement with the experimentally measured BSO bulk lattice constant equal to (4.119 Å).[55] Our B3LYP (4.234 Å)[48] and B3PW (4.234 Å)[32] computed BZO bulk lattice constants are equal, and in a much better agreement with experimental value (4.199 Å)[56] that the relevant PWGGA (4.24 Å)[47] and HF (4.25 Å)[47] calculated BZO bulk lattice constants. With aim to characterize the covalency effects, effective atomic charges as well as chemical bonding for the ABO_3 perovskites bulk, and their (001) surfaces, we used the conventional Mulliken population analysis.[57–60]

Our effective atomic charges as well as bond populations for BSO perovskite computed by means of B3LYP hybrid exchange-correlation functional are listed in Table II. Our B3LYP computed atomic charges for the BSO bulk are equal to +1.825*e* for the Ba, + 2.122*e* for the Sn atom, and −1.316*e* for the O atom. Our computed Sn atom charge in the BSO perovskite (+2.122*e*) is only slightly smaller than the Zr atom charge (+2.134*e*) in the BZO perovskite. Our B3LYP computed Sn–O chemical bond population (+0.284*e*) in BSO perovskite is 2.63 times larger than respective Zr–O bond population (+0.108*e*) in the BZO perovskite.

Our B3LYP (3.65 eV) and B3PW (3.68 eV) computed bulk Γ-Γ band gaps for BSO perovskite are in much more acceptable agreement with the experimental result of 3.1 eV[42,43] than our HF (12.11 eV) or PWGGA (1.71 eV) computation results (Table III). Experimental BZO bulk Γ-Γ band gap is equal to 5.3 eV.[45] Our PWGGA computed BZO bulk Γ-Γ band gap is very small, equal to only 3.24 eV[47] (Table III). Just opposite, exactly four times larger is our HF computed BZO bulk Γ-Γ band gap (12.96 eV)[47] (Table III). Again, almost equal, and in a fair agreement with the experiment (5.3 eV), are our B3LYP (4.79 eV)[48] and B3PW (4.93 eV)[47] (Fig. 3) computed bulk Γ-Γ band gaps.

3.2. Computation results for BSO and BZO (001) surfaces

Our B3LYP or B3PW computation results for the upper three-layer atomic relaxations of BO_2 or BaO-terminated BSO and BZO perovskite (001) surfaces are given in Tables IV and V. As it possible to see from Tables IV and V, in most cases the BSO and BZO perovskite BO_2 and BaO-terminated (001) surface upper layer

TABLE I. B3LYP, B3PW, PWGGA, and HF computed bulk lattice constants (in Å) for the BSO and BZO perovskite bulk. The experimental data (in Å) are listed for comparison .

Perovskite	Functional	Computed	Experimental
BSO	B3LYP	4.107	4.119[55]
	B3PW	4.087	
	PWGGA	4.107	
	HF	4.078	
BZO	B3LYP	4.234[48]	4.199[56]
	B3PW	4.234[32]	
	PWGGA	4.24[47]	
	HF	4.25[47]	

TABLE II. Our B3LYP or B3PW computed effective atomic charges *Q* (in *e*) as well as bond populations *P* (in *e*) in BSO and BZO perovskites.

Bulk material		BSO	BZO
Ion	Property	B3LYP	B3PW
A	*Q*	+1.825	+1.815
	P	−0.030	−0.012
O	*Q*	−1.316	−1.316
	P	+0.284	+0.108
B	*Q*	+2.122	+2.134

TABLE III. B3LYP, B3PW, PWGGA, and HF computed bulk Γ-Γ band gaps (in eV) for BSO and BZO perovskites[42,43,45,47,48]. Experimental BSO and BZO bulk Γ-Γ band gaps are listed for comparison purpose (in eV)[42,43,45]

Perovskite	Method	Γ-Γ band gap, bulk	Experiment
BSO	B3LYP	3.65	3.1[42,43]
	B3PW	3.68	
	PWGGA	1.71	
	HF	12.11	
BZO	B3LYP	4.79[48]	5.3[45]
	B3PW	4.93[47]	
	PWGGA	3.24[47]	
	HF	12.96[47]	

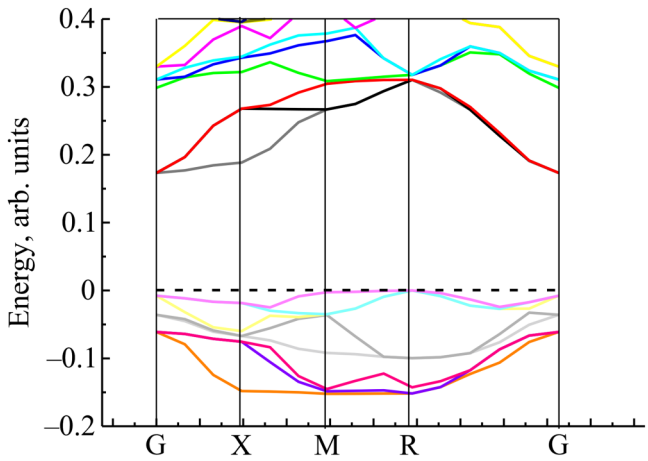

FIG. 3. Our B3PW computed electronic band structure for BZO bulk.

TABLE IV. Our B3LYP or B3PW computed atomic relaxation (% of a_0) for BO_2-terminated BSO and BZO (001) surfaces.

Bulk material		BSO	BZO
Termination for (001) surface		SnO_2	ZrO_2
Layer	Ion	B3LYP	B3PW
1	B	−0.97	−1.79
	O	−0.27	−1.70
2	Ba	+0.93	+1.94
	O	−0.04	+0.85
3	B	−0.11	−0.03
	O	+0.03	0.00

TABLE V. Our B3LYP or B3PW computed atomic relaxation (% of a_0) for BaO-terminated BSO and BZO (001) surfaces.

Bulk material		BSO	BZO
Termination for (001) surface		BaO	BaO
Layer	Ion	B3LYP	B3PW
1	Ba	−1.75	−4.30
	O	−0.39	−1.23
2	B	+0.39	+0.47
	O	−0.07	+0.18
3	Ba	−0.20	−0.01
	O	+0.02	−0.14

TABLE VI. Our B3LYP or B3PW computed surface rumpling s and relative displacements Δd_{ij} (% of a_0) for the three near-surface planes.

		BaO-terminated (001) surface			BO_2-terminated (001) surface		
Material	Method	s	Δd_{12}	Δd_{23}	s	Δd_{12}	Δd_{23}
BSO	B3LYP	+1.36	−2.14	+0.59	+0.70	−1.90	+1.04
BZO	B3PW	+3.07	−4.77	+0.48	+0.09	−3.73	+1.97

TABLE VII. B3LYP and B3PW computed B–O chemical bond populations in BSO and BZO perovskite bulk and on their BO_2-terminated (001) surfaces (in e) .

		B–O chemical bond population	
Perovskite	Functional	ABO_3 bulk	BO_2-term. (001)
BSO	B3LYP	0.284	0.298
BZO	B3PW	0.108	0.132

atoms relax inwards, the second surface layer atoms relax outwards, whereas the third surface layer atoms, again, relax inwards. For BaO and BO_2-terminated BSO and BZO perovskite (001) surface upper two layers, the metal atom relaxation magnitudes always are considerably larger than the respective oxygen atom relaxation magnitudes.

The largest relaxation magnitude between all upper and second layer metal atoms exhibit the BaO-terminated BZO (001) surface upper layer Ba atom equal to −4.30% of a_0.

Additionally, we also computed and listed in Table VI the surface rumpling s and the changes in the interlayer distances Δd_{12} and Δd_{23} for completely relaxed BSO and BZO perovskite (001) surfaces (Tables IV and V).

According to our B3PW computations, the BaO-terminated BZO (001) surface rumpling (3.07% of a_0) is more than two times larger than the BaO-terminated BSO (001) surface rumpling (1.36% of a_0). Just opposite, the SnO_2-terminated BSO (001) surface rumpling (+0.70% of a_0) is almost eight times larger than the respective ZrO_2-terminated BZO (001) surface rumpling (+0.09% of a_0) (Table VI). The systematic trend for both BSO and BZO perovskite BaO and BO_2-terminated (001) surfaces is contraction of the interlayer distance (Δd_{12}) and expansion of the interlayer distance (Δd_{23}) (Table VI).

The systematic trend, as it is possible to see from Table VII, is the increase in the B–O chemical bond covalency near the BO_2-terminated BSO and BZO (001) surfaces in comparison with the bulk values. For example, the B3LYP computed B–O chemical bond covalency in the BSO bulk is already very large (0.284e) and is increased till 0.298e near the SnO_2-terminated BSO (001) surface. Just opposite, the BZO bulk B–O chemical bond covalency is much smaller than in the BSO perovskite, only +0.108e. Also, the BZO perovskite B–O chemical bond covalency is increased near the ZrO_2-terminated BZO (001) surface (0.132e), in comparison with bulk value (+0.108$_e$) (Table VII).

As can be seen from Table VIII, our B3PW computed ZrO_2-terminated BZO (001) surface energy is 1.31 eV. It is almost identical with our B3PW computed BaO-terminated BZO (001) surface energy equal to 1.30 eV.

TABLE VIII. B3PW computed surface energies (in eV) for ZrO_2 and BaO-terminated BZO (001) surfaces.

Termination	(001) surface energy
ZrO_2	1.31
BaO	1.30

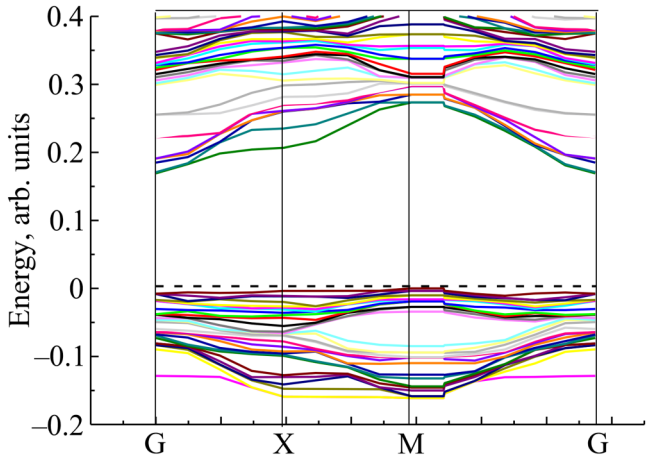

FIG. 4. Our B3PW computed electronic band structure for BaO-terminated BZO (001) surface.

TABLE IX. B3PW computed BZO perovskite bulk as well as BaO and ZrO_2-terminated (001) surface Γ-Γ band gaps (in eV). Experimental Γ-Γ band gap value is listed for comparison (in eV).

BZO, B3PW	Γ-Γ band gap
Bulk	4.93
BaO-terminated BZO (001) surface	4.82
ZrO_2-terminated BZO (001) surface	4.48
Experiment	5.3[45]

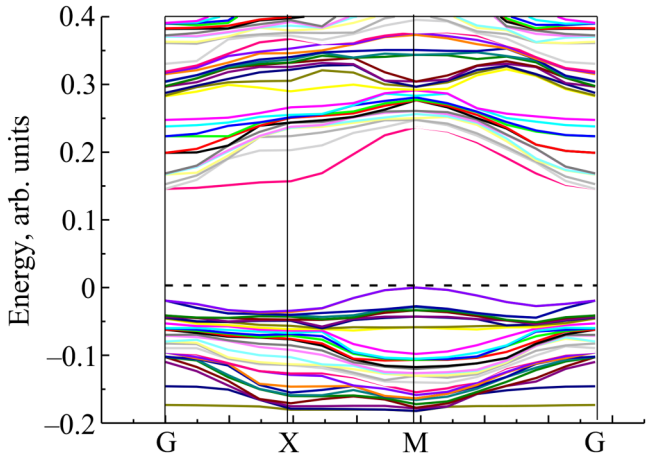

FIG. 5. Our B3PW computed electronic band structure for ZrO_2-terminated BZO (001) surface.

As it is possible to see from Figs. 4 and 5 as well as Table IX, the B3PW computed BZO bulk Γ-Γ band gap is 4.93 eV. This BZO bulk Γ-Γ band gap is reduced near the BaO-terminated BZO (001) (4.82 eV) (Fig. 4) as well as near the ZrO_2-terminated BZO (001) surface (4.48 eV) (Fig. 5).

4. CONCLUSIONS

We performed *ab initio* computations for BSO and BZO perovskite (001) surfaces using the B3PW and B3LYP hybrid exchange-correlation functionals. For our computed BSO and BZO perovskite (001) surfaces, with only a few exceptions, all atoms of the upper surface layer relax inwards, whereas all atoms of the second surface layer relax outwards, and, again, all third layer atoms relax inwards. The relaxation of BSO and BZO (001) surface metal atoms for upper two surface layers, for both BaO and BO_2-terminations, generally are remarkably larger than the relaxation of relevant oxygen atoms. The BaO (1.30 eV) and ZrO_2-terminated (1.31 eV) BZO (001) surface energies are nearly equal. It means, that both BaO and ZrO_2-terminated BZO (001) surfaces can co-exist in BZO perovskite. The BZO perovskite BaO (4.82 eV) and ZrO_2-terminated (4.48 eV) (001) surface Γ-Γ band gaps are decreased with respect to the respective bulk Γ-Γ band gap value equal to 4.93 eV. The B–O chemical bond populations in BSO and BZO perovskite bulk (0.284*e* and 0.108*e*) always are smaller than near their SnO_2 and ZrO_2-terminated (001) surfaces (0.298*e* and 0.132*e*), respectively.

ACKNOWLEDGMENTS

This study was partially supported by the Latvian Council of Science Grant Number: LZP-2021/1-464.

REFERENCES

[1]R. I. Eglitis and D. Vanderbilt, Phys. Rev. B **76**, 155439 (2007).
[2]B. Meyer and D. Vanderbilt, Phys. Rev. B **63**, 205426 (2001).
[3]M. Dawber, K.M. Rabe, and J. F. Scott, "Physics of thin-film ferroelectric oxides," Rev. Mod. Phys. **77**, 1083 (2005).
[4]N. Porotnikova, A. Farlenkov, S. Naumov, M. Vlasov, A. Khodimchuk, A. Fetisov, and M. Ananyev, Phys. Chem. Chem. Phys. **23**, 11272 (2021).
[5]W. D. Mesquita, S. R. Jesus, M. C. Oliveira, R. A. P. Ribeiro, M. R. C. Santos, M. G. Junior, E. Longo, and M. F. C. Gurgel, Theor. Chem. Acc. **140**, 27 (2021).
[6]S. Piskunov and R. I. Eglitis, Solid State Ionics **274**, 29 (2015).
[7]E. A. Kotomin, S. Piskunov, Y. F. Zhukovskii, R. I. Eglitis, A. Gopejenko, and D. E. Ellis, Phys. Chem. Chem. Phys. **10**, 4258 (2008).
[8]M. G. Brik, C. G. Ma, and V. Krasnenko, Surf. Sci. **608**, 146 (2013).
[9]R. I. Eglitis, J. Purans, A. I. Popov, and R. Jia, Symmetry **13**, 1920 (2021).
[10]R. A. P. Ribeiro, M. C. Oliveira, A. G. Souza, M. R. D. Bomio, F. V. Motta, L. Gracia, S. R. Lazaro, E. Longo, and J. Andrés, J. Appl. Phys. **126**, 235301 (2019).
[11]L. Grigorjeva, D. K. Millers, V. Pankratov, R. T. Williams, R. I. Eglitis, E. A. Kotomin, and G. Borstel, Solid State Commun. **129**, 691 (2004).
[12]H. J. Chun, Y. Lee, S. Kim, Y. Yoon, Y. Kim, and S. C. Park, Appl. Surf. Sci. **578**, 152018 (2022).
[13]R. Eglitis, A. I. Popov, J. Purans, and R. Jia, Fiz. Nizk. Temp. **46**, 1418 (2020) [Low Temp. Phys. **46**, 1206 (2020)].
[14]Y. Si, H. Liu, H. Yu, X. Jiang, and D. Sun, Surface and Coatings Technology **431**, 128008 (2022).
[15]R. I. Eglitis, E. A. Kotomin, and G. Borstel, J. Phys. Condens. Matter **12**, L431 (2000)

[16]M. A. Qaiser, X. Z. Ma, R. Ma, W. Ali, X. Xu, G. Yuan, and L. Chen, J. Am. Ceram. Soc. **102**, 5424 (2019).
[17]P. M. Bulemo and I. D. Kim, J. Korean Ceram. Soc. **57**, 24 (2020).
[18]N. N. Toan, S. Saukko, and V. Lanto, Physica B: Condensed Matter **327**, 279 (2003).
[19]V. Lantto, S. Saukko, and N. N. Toan, J. Electroceram. **13**, 721 (2004).
[20]A. Benali, S. Azizi, M. Bejar, E. Dhahri, and M. F. P. Graca, Ceram. Internat. **40**, 14367 (2014).
[21]W. Haron, A. Wisitsoraat, and S. Wongnawa, Ceram. Internat. **43**, 5032 (2017)
[22]L. Sun, H. Qin, K. Wang, M. Zhao, and J. Hu, Materials Chemistry and Physics **125**, 305 (2011).
[23]J. Meng, Z. Lan, and Q. Lin, J. Mater. Sci. **54**, 1967 (2019).
[24]Y. X. Wang, M. Arai, T. Sasaki, and C. L. Wang, Appl. Phys. Lett. **88**, 091909 (2006).
[25]R. A. Evarestov and A. V. Bandura, Solid State Ionics **188**, 25 (2011).
[26]R. I. Eglitis, J. Purans, A. I. Popov, D. Bocharov, A. Chekhovska, and R. Jia, Symmetry **14**, 1050 (2022).
[27]M. Arrigoni, T. S. Bjorheim, E. Kotomin, and J. Maier, Phys. Chem. Chem. Phys. **18**, 9902 (2016).
[28]J. Ho, E. Heifets, and B. Merinov, Surf. Sci. **601**, 490 (2007).
[29]J. S. Kim, J. H. Yang, B. K. Kim, and Y. C. Kim, Solid State Ionics **275**, 19 (2015).
[30]A. V. Bandura, R. A. Evarestov, and D. D. Kuruch, Surf. Sci. **604**, 1591 (2010).
[31]S. M. Saeed, T. Norby, and T. S. Bjorheim, J. Phys. Chem. C **123**, 20808 (2019).
[32]R. I. Eglitis, J. Phys. Condens. Matter **19**, 356004 (2007).
[33]Y. Wang, Z. Zhang, Y. Wang, E. Doan, L. Yuan, W. Tang, and K. Yang, Vacuum **212**, 111977 (2023).
[34]W. J. Lee, H. Lee, K. T. Ko, J. Kang, H. J. Kim, T. Lee, J. H. Park, and K. H. Kim, Appl. Phys. Lett. **111**, 231604 (2017).
[35]W. H. Lee, H. J. Kim, E. Sohn, T. H. Kim, J. Y. Park, W. Park, H. Jeong, T. Lee, J. H. Kim, K. Y. Choi, and K. H. Kim, Appl. Phys. Lett. **108**, 082105 (2016).
[36]Y. Li, Y. Wang, Y. Huang, X. Liu, L. Yuan, and K. Yang, ACS Appl. Nano Mater. **7**, 11995 (2024).
[37]P. Y. Chen, C. H. Lam, B. Edmondson, A. B. Posadas, A. A. Demkov, and J. G. Ekerdt, J. Vac. Sci. Technol. A **37**, 050902 (2019).
[38]A. Prakash, J. Dewey, H. Yun, J. S. Jeong, K. A. Mkhoyan, and B. Jalan, J. Vac. Sci. Technol. A **33**, 060608 (2015).
[39]H. Takashima and Y. Inaguma, Appl. Phys. Lett. **111**, 091903 (2017).
[40]A. Prakash, P. Xu, X. Wu, G. Haugstad, X. Wang, and B. Jalan, J. Mater. Chem. C **5**, 5730 (2017).
[41]Y. Wang, R. Sui, M. Bi, W. Tang, and S. Ma, RSC Adv. **9**, 14072 (2019).
[42]M. A. Janifer, S. Anand, C. J. Prabagar, and S. Pauline, Materials Today: Proceedings **47**, 2067 (2021).
[43]H. J. Kim, V. Kim, T. H. Kim, H. M. Kim, B. G. Jeon, W. J. Lee, H. S. Mun, K. T. Hong, J. Yu, K. Char, and K. H. Kim, Phys. Rev. B **86**, 165205 (2012).
[44]K. S. Knight, J. Mater. Sci. **55**, 6417 (2020).
[45]J. Robertson, J. Vacuum. Sci. Technol. **18**, 1785 (2000).
[46]R. Dovesi, R. Orlando, C. Roetti, C. Pisani, and V. R. Saunders, Physica Status Solidi B **217**, 63 (2000).
[47]R. I. Eglitis and A. I. Popov, J. Saudi Chem. Soc. **22**, 459 (2018).
[48]R. I. Eglitis, Solid State Ionics **230**, 43 (2013).
[49]R. Dovesi, V. R. Saunders, C. Roetti, R. Orlando, C. M. Zicovich-Wilson, F. Pascale, B. Civalleri, K. Doll, N. M. Harrison, I. J. Bush, Ph. D'Arco, M. Llunel, M. Causá, Y. Noël, L. Maschio, A. Erba, M. Rérat, and S. Casassa, *CRYSTAL-2017 User Manual* (University of Torino, Italy, 2017).
[50]S. Piskunov, E. Heifets, R. I. Eglitis, and G. Borstel, Comput. Mater. Sci. **29**, 165 (2004).
[51]J. P. Perdew and Y. Wang, Phys. Rev. B **33**, 8800 (1986); *Erratum* in Phys. Rev. B **40**, 3399 (1989).
[52]J. P. Perdew and Y. Wang, Phys. Rev. B **45**, 13244 (1992).
[53]C. Lee, W. Yang, and R. G. Parr, Phys. Rev. B **37**, 785 (1988).
[54]H. J. Monkhorst, "Special points for brillouin-zone integrations," Phys. Rev. B **13**, 5188 (1976).
[55]J. C. Farfán, J. A. Rodríguez, F. Fajardo, E. V. López, D. A. Landínez Téllez, and J. Roa-Rojas, Physica B: Condensed Matter **404**, 2720 (2009).
[56]M. D. Mathews, E. B. Mirza, and A. C. Momin, J. Mater. Sci. Lett. **10**, 305 (1991).
[57]E. R. Davidson and A. E. Clark, Int. J. Quantum Chem. **122**, e26860 (2022).
[58]B. Zulueta, S. V. Tulyani, P. R. Westmoreland, M. J. Frisch, E. J. Petersson, G. A. Petersson, and J. A. Keith, J. Chem. Theory Comput. **18**, 4774 (2022).
[59]T. Kaneko and K. Sodeyama, Chem. Phys. Lett. **762**, 138199 (2021).
[60]J. Hu, X. Jian, T. Yang, and X. Peng, Diamond and Related Materials **123**, 108864 (2022).